Conf-9506130--1

UCRL-JC-121272
PREPRINT

Performance of the Beamlet Laser, A Testbed for the National Ignition Facility

B. M. Van Wonterghem, J. A. Caird, C. E. Barker,
J. H. Campbell, J. R. Murray, D. R. Speck

This paper was prepared for submittal to the
Laser Optics '95
St. Petersburg, Russia
June 27 - July 1, 1995

June 19, 1995

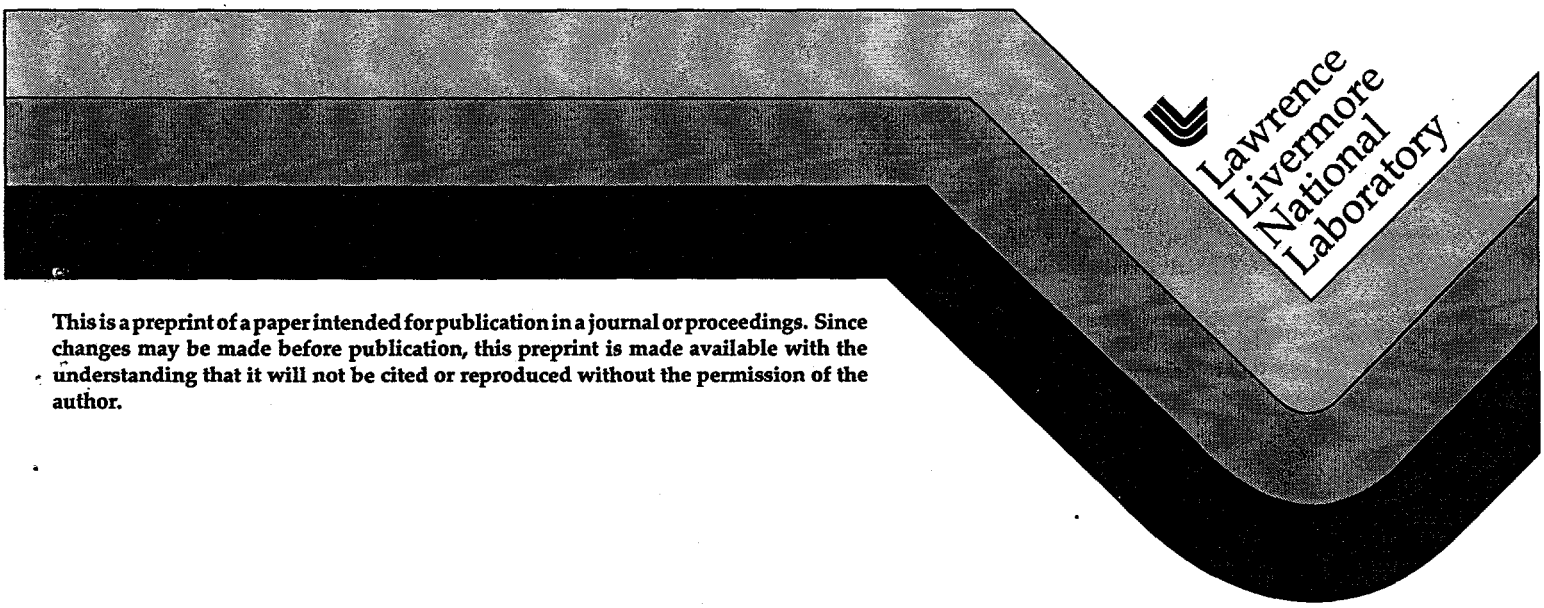

Performance of the Beamlet laser, a testbed for the national ignition facility

B. M. van Wonterghem, J. A. Caird, C. E. Barker,
J. H. Campbell, J. R. Murray, and D. R. Speck

University of California
Lawrence Livermore National Laboratory
P.O. Box 5508, L-490
Livermore, CA 94551, U. S. A.
(510)422-6152, fax (510)422-7748

ABSTRACT

We present initial performance studies for Beamlet, a single-beam prototype for megajoule-class neodymium-glass laser fusion drivers using a multipass main amplifier, adaptive optics, and efficient, high-fluence conversion to the third harmonic. The Beamlet final amplifier uses Brewsters-angle glass slabs with a square 39x39 cm^2 aperture and a full-aperture plasma-electrode Pockels cell switch. The laser has been tested at the fundamental wavelength over a range of pulselengths from 1-10 ns up to energies of 5.8 kJ at 1 ns and 17.3 kJ at 10 ns at a beam area of 35 x 35 cm^2. A 39-actuator deformable mirror system corrects the beam to a Strehl ratio of 0.4.

Keywords: neodymium glass lasers, inertial confinement fusion

1. INTRODUCTION

The United States Department of Energy has proposed building a National Ignition Facility (NIF) for Inertial Confinement Fusion (ICF) with the goal of demonstrating ignition and propagation of a thermonuclear fusion burn. This facility would irradiate fusion targets with shaped puses of 1.8 MJ in 3.5 ns using the 350-nm third harmonic of a large neodymium glass laser. The Commissariat a l'Energie Atomique of France has proposed building a Laser Megajoule of similar size and design, and other smaller but still large laser facilities have been proposed elsewhere.

It is important to operate large, expensive laser systems such as these at the highest acceptable average fluence, since the average fluence determines the total beam area required and the cost of the laser is roughly proportional to that area. The fluence in the system is limited by damage to small defects in the optical components in the regions of peak fluence, so we must minimize the ratio of peak to average fluence in the beam. The NIF laser, like other large glass lasers, uses vacuum relay telescopes to reimage a very flat input intensity profile at several points through the laser chain[1]. The effective optical propagation distance from the original flat profile is reset to zero at each image, so diffractive noise growth is minimized by this strategy. High-spatial-frequency noise (which can see exponential growth at very high intensities) is also reset to zero by blocking high-spatial-frequency noise at the position where the beam comes to a focus in the relay telescope. The NIF laser will operate at significantly higher fluence than most existing large laser systems to take advantage of the improved component damage thresholds that have become available in recent years[2].

The driver for the proposed NIF would be a laser system containing 192 individual "beamlets" having an amplifier clear aperture of 40 cm and beams a few centimeters smaller. The Brewster's-angle glass amplifier slabs for these beamlets are in four large amplifier arrays stacked four high and twelve wide. The baseline laser design is a four-pass multipass main amplifier with a full-aperture plasma-electrode Pockels cell switch and frequency conversion to the third harmonic. The design differs from previous large glass lasers in that it uses multiple passes through a single large amplifier stage to go from an injected energy of order 1 J to an output of order 10 kJ, rather than numerous intermediate amplifiers of increasing size. The multipass design greatly reduces the number of components and hence the cost of the system.

A full-scale prototype ("Beamlet") of a single aperture of the proposed NIF laser has been assembled at LLNL to test the performance of the laser design proposed for that system.

2. Architecture of the Beamlet multipass final amplifer stage

Figure 1 shows a schematic diagram of the final amplifier stage of the Beamlet laser. An input

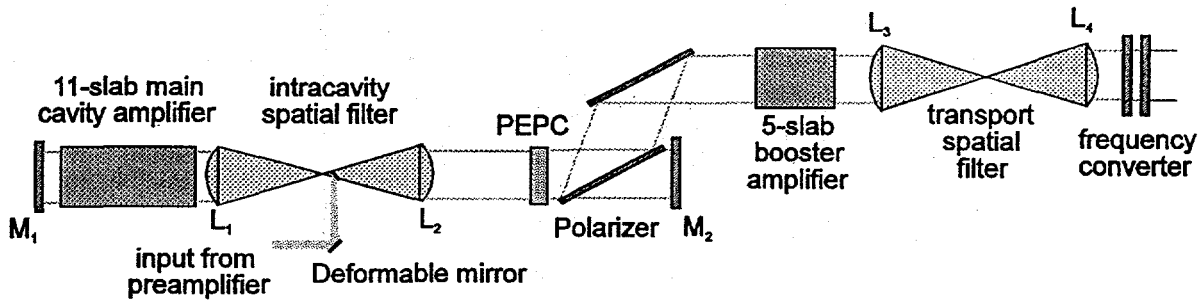

Figure 1. Schematic diagram of the Beamlet main amplifier stage. PEPC is a plasma-electrode Pockels cell.

pulse of order 1 J from the preamplifier strikes a deformable mirror used to control the output wavefront and comes to a focus at the central plane of a large intracavity vacuum spatial filter. The beam expands past focus, is recollimated by lens L_1, and makes two passes through an 11-slab-long main cavity amplifier, emerging at an energy of order 100 J. It makes another transit through the intracavity spatial filter at a small angle to the injected beam, missing the small mirror (2x2 cm) that was used to inject that beam. Meanwhile the plasma-electrode Pockels cell PEPC fires to rotate the beam polarization so that it passes through a thin-film polarizer and reflects from M_2. The beam returns through the intracavity spatial filter and makes another double pass through the main cavity amplifier. While it is in transit, the Pockels cell returns to its off state so that the beam reflects from the polarizer when it returns at an energy of order 5 kJ. The beam the makes a single pass through a 5-slab-long booster amplifier, emerging with an energy of order 10 kJ. The output beam then passes through a second spatial filter and proceeds on to frequency conversion and output beam diagnostics. We have run several beam sizes during these initial experiments, ranging from 29.6 to 35 cm square, as limited by the size of the crystals available.

3. Discussion of specific components

3.1 Main amplifier

The Beamlet main amplifier slabs are Schott LG750 glass with 3.5 x 10^{20}/cm^3 Nd^{3+} doping are 78.3 x 44.4 x 4 cm^3 finished size with absorbing edge claddings. The amplifier clear aperture is 39 x 39 cm^2, or slightly less than proposed for NIF. The amplifiers for NIF are stacked in a close-packed array with long flashlamps pumping multiple slabs, as mentioned previously. The Beamlet amplifiers have been constructed as an array of beamlet apertures stacked two high and two wide in order to demonstrate some of the design features of such amplifier arrays, however only one of the amplifier apertures contains high quality laser glass and is used in the system.

The amplifier aperture is large enough that amplified spontaneous emission causes the gain to decrease by about 15% from the center to the ends of the long slab dimension. We compensate for this gain rolloff by shaping the input beam from the preamplifier to be more intense at the edges so that the output beam will have uniform average intensity. This strategy allows us to use a larger amplifier aperture, thereby reducing the number of beamlets in a large system and reducing the overall system cost.

3.2 Plasma-electrode Pockels cell

The plasma electrode Pockels cell (PEPC)[3,4] uses the longitudinal electrooptic effect in a 36 x 36 cm^2 clear aperture by 1 cm thick plate of the crystal potassium dihydrogen phosphate (KDP) to rotate the beam polarization at full aperture. It is necessary to have conducting electrodes on the crystal surface to use the crystal in this way, and those electrodes must have a very high laser damage threshold to pass the high-fluence beam.

Figure 2 shows how this can be accomplished. Two plasma pulsers generate helium plasmas on both faces of the crystal, and then a switch pulser applies a differential voltage between the two plasmas to charge the faces of the crystal. We find that under typical operation the PEPC will switch 6 kJ out of the laser cavity with a residual leakage through the polarizer of about 30 J. All optical surfaces in the Pockels cell are antireflection coated using a silica sol-gel process, and these coatings are unaffected by the plasma.

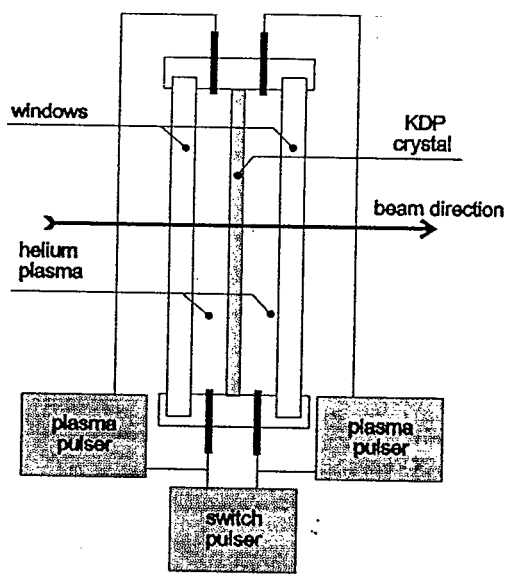

Figure 2. Plasma-electrode Pockels cell

3.3 Oscillator and preamplifier system

The oscillator and preamplifier ("front end") for a large ICF laser must allow highly flexible pulse shaping and beam balancing between different beamlets. Also the oscillator must be phase-modulated to a bandwidth of ~30GHz in a system of this size to prevent transverse stimulated Brillouin scattering in the large, high-fluence components at the output of the chain[5]. Current large lasers use mechanical adjustments and modulators running at high voltages for these functions. For NIF we propose s more flexible system based on modulators and components developed for high-speed fiber optic communication networks, with a fiber carrying a shaped pulse to a separate preamplifier for each beamlet located near the injection point into the spatial filter. Beamlet has a front end based on this technology.

A pulse from a low-power diode-pumped laser is injected into a single-mode optical fiber. This fiber goes to a lithium niobate integrated-optics modulator having one phase and two amplitude modulator sections to generate phase-modulated, high-contrast pulses at a power level of a few tenths of a watt. The amplitude modulator has a risetime of 75 ps. The output from the modulator travels over 60 m of single-mode fiber to a high-gain regenerative ring preamplifier[6] that boosts the pulse energy to about 10 mJ. The pulse is then reshaped to give the desired square shape and intensity profile, and further amplified to of order 1 J in a four-pass glass rod amplifier. It then passes to the main amplifier stage shown in Figure 1.

3.4 Adaptive optics system

Beamlet has a deformable mirror and a Hartmann wavefront sensor in the output beam diagnostics package for control of the output laser wavefront using technology developed for a large dye laser system[7]. The mirror has 39 electrostrictive actuators forming an array of equilateral triangles slightly larger than the 5 x 5 cm^2 beam footprint on the mirror, and its location in the system is shown in Figure 1. It can correct up to ±5 waves of low order aberrations at the laser wavelength. The Hartmann sensor uses a 77-element lenslet array and a standard television CCD camera to acquire an output wavefront.

The adaptive optics system operates in a preset mode at present. The control loop is closed using 1/4 Hz pulses from the front end, or using a CW alignment laser, and the wavefront error due to static optical errors and long-term thermal distortions is corrected. The mirror is then frozen in position several minutes before a shot. There is some prompt thermal distortion induced by firing the flashlamps in the main amplifier which is not corrected under these conditions. This distortion can be extracted from the wavefront measured on a previous shot and added to the preset wavefront on the mirror. There remains some distortion due to convection cells in the air path that cannot be corrected using adaptive optics in this mode.

3.5 Frequency converter

The Beamlet frequency conversion design and performance are discussed in a companion paper in this volume.

4. Laser performance

4.1 Stage gain of the main amplifier stage

Figure 4 shows a plot of energy output as a function of input for the Beamlet main amplifier stage, compared to a saturation model for the system. The highest energy shot we have fired to date was 17.3 kJ at 10 ns in a beam with zero-intensity points at 35 x 35 cm^2. The input for that shot was 1.9 J with an intensity profile rising by a factor of 15 during the pulse to give a square output with heavily-saturated amplifiers.

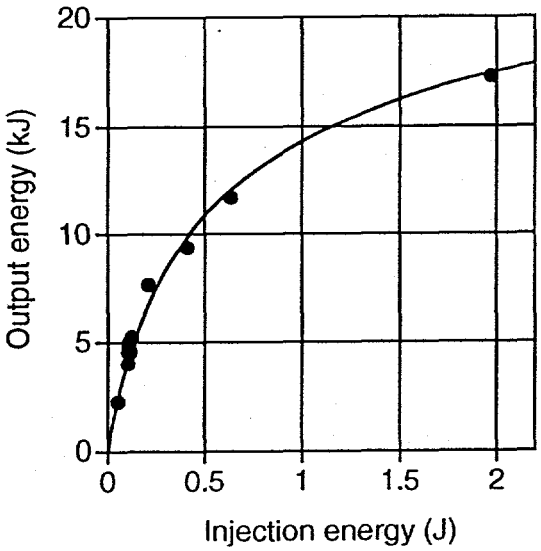

Figure 3. Stage gain (output vs. input) of the Beamlet main amplifier stage.

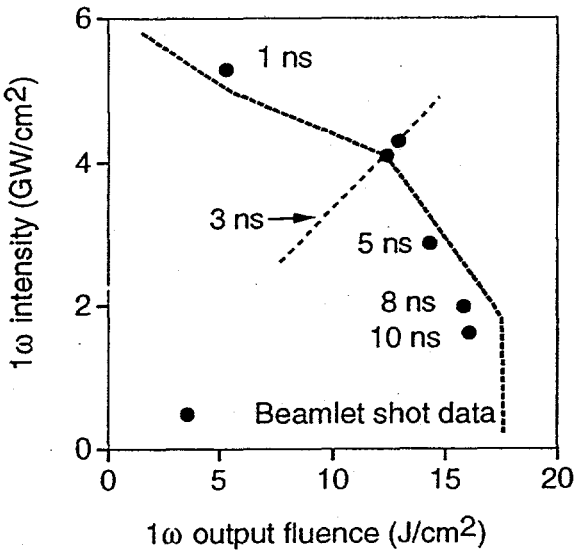

Figure 4. Operating range of Beamlet in irradiance/fluence space. The dots are the six shots from this test series closest to the maximum safe operating limit.

4.2 Average irradiance and fluence demonstrated in this test series

Figure 3 shows a plot of average laser irradiance versus fluence at the output of the Beamlet laser system, showing the operating range that we have explored during this initial test series. Note that square output pulses of constant pulselength but different energy (which is our usual operating condition for these tests) lie on a straight line through the origin in a plot such as this, such as the light dashed line shown for 3 ns square pulses. The heavy dashed line shows our projection for maximum safe operating limits based on the damage thresholds measured for typical components. At high irradiance and low fluence, the laser is limited by nonlinear growth of intensity modulation through the booster amplifier that then leads to damage in the high-fluence components at the output of the laser. Over the intermediate range of pulselengths, the limit switches over to a combination of nonlinear growth in the large cavity amplifier and damage to the polarizer, which has the lowest damage threshold of any component in the main laser cavity. For very long pulses at high fluence the stored energy is extracted so efficiently that the pulse distortion is very high and the input pulse must rise to an unreasonable intensity at the end of the pulse to maintain a square output pulse. A typical ignition target for a large facility such as NIF requires a shaped pulse with a long leading foot and an intense final pulse with a width of about 3.5 ns. From a laser damage point of view, these pulses

resemble 4-5 ns square pulses of the same irradiance and fluence. The irradiance and fluence demonstrated in these tests on Beamlet are slightly above those proposed as nominal operating conditions for the NIF. We have not seen serious laser damage to clean components as a consequence of 350 laser shots, of which 35-40 shots were near the expected maximum safe operating conditions for the system. There is some minor damage to the polarizer, and we have also seen damage to lens L_3 as a consequence of contaminants from the vacuum system depositing on the vacuum side of that lens. This will have to be corrected.

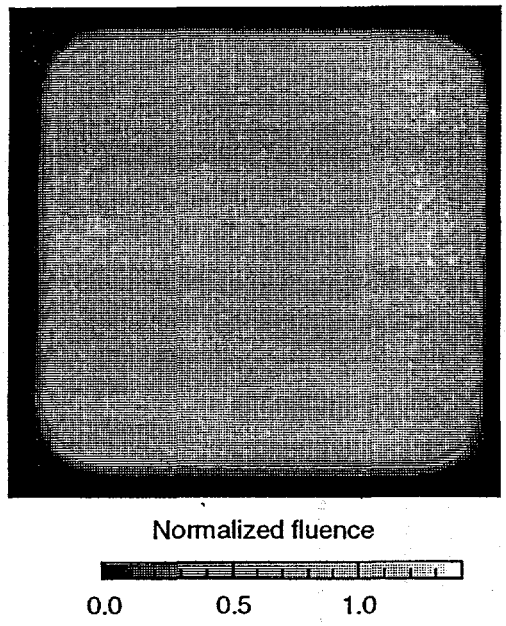

Figure 5. Near-field intensity distribution of the Beamlet output beam.

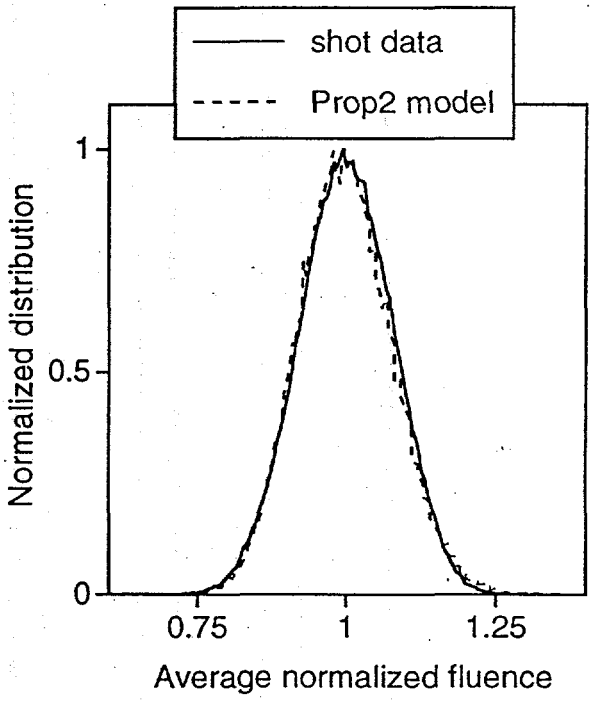

Figure 6. Intensity distribution in the beam of Figure 5 compared to the distribution predicited by a propagation model.

4.3 Output intensity profile

It is important to minimize intensity noise on the beam and to fill the laser aperture as uniformly as possible to maximize the energy we can extract from a given area. Figure 5 shows an output beam photograph of a high-energy shot on Beamlet (12.4 J/cm^2 , 3-ns square output pulse). Figure 6 is a plot of pixel intensities from the flat-top central region of this beam showing that the most intense points on the beam are at about 1.3 times the average fluence. A computer code that simulates diffractive propagation in laser systems projects similar levels of intensity noise on the beam, as also shown in the figure. The code assumes optical distortions on the components similar to those we have measured for Beamlet components. The fill factor of this beam, defined as (area containing full beam energy at fluence in the flat-top region) divided by (area at zero intensity), is 88% for typical images.

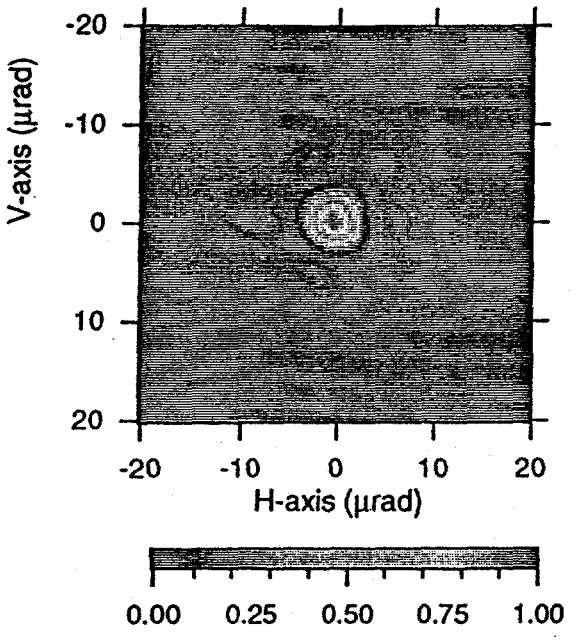

Figure 7. Far-field intensity distribution of the Beamlet beam with aberrations corrected.

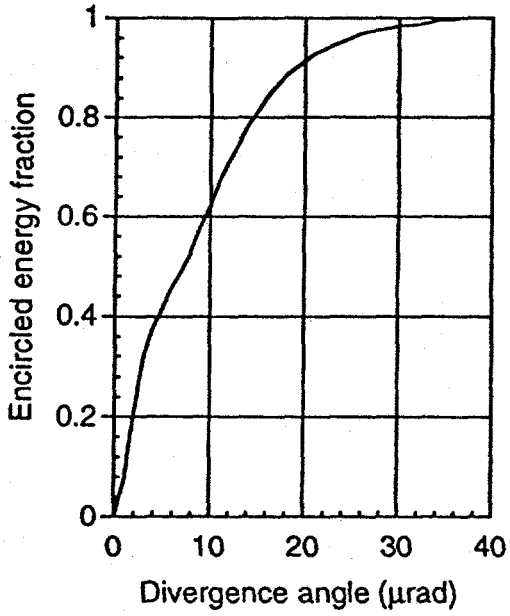

Figure 8. Encircled energy fraction of the beam in Fig. 7 as a function of half-angle (radius) in the far-field.

4.4 Far-field energy distribution using adaptive optics

A typical fusion ignition target for NIF will require a spot size corresponding to a far-field angular distribution of ±35 microradians, which is large compared to the ~±4.5-microradian diffraction limit of a 35-cm aperture beam. There are some users who would like smaller spots, however, and also it is possible to reduce the cost of some optical components and increase the laser shot rate if we can accept higher distortions in the system. Therefore it is important to understand how well we might correct the beam for NIF with a modest adaptive optics system.

Figure 7 shows the far-field distribution of the Beamlet beam with about 2.5 waves (peak to valley) of static and long term thermal aberrations and about 1.5 waves of prompt thermal aberrations induced by the flashlamps corrected as described in section 3.4. A completely uncorrected shot gives a far-field distribution with several lobes and a diameter of 20-30 microradians. These plots can be slightly misleading, since low intensity parts of the beam outside the prominent central diffraction-limited maximum occupy a large area and can contain a significant fraction of the energy. Figure 8 is an integral of the energy fraction inside a given radius in the far field, showing that the central diffraction maximum contains about 33% of the beam energy as compared to 82% for a perfect plane wave, or a Strehl ratio of about 0.4. This agrees with the wavefront measurement of 0.18 waves rms (0.96 waves peak-to-valley) reported by the Hartmann sensor. These measurements are for a thermally-stabilized system and the performance is somewhat worse if the amplifiers are warm and convection cells are present.

5. Conclusion

These tests show that large, multipass neodymium-glass lasers such as those proposed for the National Ignition Facility and Laser Megajoule can be built and that their performance will be in agreement with models and predictions. The tests demonstrate that a modest adaptive optics system is very useful in such systems, and can correct the output beam to near the diffraction limit. The Beamlet will now proceed to more detailed study of engineering issues for such large laser systems, such as beam smoothing techniques, long term operations and maintenance, and target optics design and performance.

6. Acknowledgements

This work was performed under the auspices of the United States Department of Energy by Lawrence Livermore National Laboratory under contract number W-7405-ENG-48.

7. References

1. W. W. Simmons, J. T. Hunt, and W. E. Warren, "Light propagation through large laser systems," *IEEE J. Quantum Electron.* **QE-17**, 1727-1744 (1981).
2. J. H. Campbell, F. Rainer, M. R. Kozlowski, C. R. Wolfe, I. M. Thomas, and F. P. Milanovich, "Damage-resistant optics for a megajoule solid-state laser, " *Proc. SPIE,* vol. **1441**, *Laser-induced damage in optical materials 1990*, 444-456 (1990).
3. J. Goldhar and M. A. Henesian, "Large=aperture electrooptical switches with plasma electrodes," *IEEE J. Quantum Electron.*, **QE-22**, 1137-1147 (1986).
4. M. A. Rhodes, B. Woods, J. J. DeYoreo, D. Roberts, and L. J. Atherton, "Performance of large-aperture optical switches for high-energy ICF lasers," LLNL preprint UCRL-JC-118537, to be published in *Applied Optics*.
5. J. R. Murray, J. R. Smith, R. B. Ehrlich, D. T. Kyrazis, C. E. Thompson, T. L. Weiland, and R. B. Wilcox, "Experimental observation and suppression of transverse stimulated Brillouin scattering in large optical components," *J. Opt. Soc. Am. B* **6**, 2402-2411 (1989).
6. F. Patterson and M. D. Perry, "Design and performance of a multiterawatt subpicosecond neodymium glass laser," *J. Opt. Soc. Am. B* **8**, 2384-2391 (1991).
7. J. T. Salmon, E. S. Bliss, T. W. Long, E. L. Orham, R. W. Presta, C. D. Swift, and R. S. Ward, "Real-time wavefront correction system using a zonal deformable mirror and a Hartmann sensor," *Proc. SPIE*, vol. **1542** *Active and adaptive optical systems*, 459-467 (1991).